

Vascular compromise and hemodynamics in pulmonary arterial hypertension: Model predictions

Zoheir Bshouty MD PhD FRCPC

Z Bshouty. Vascular compromise and hemodynamics in pulmonary arterial hypertension: Model predictions. *Can Respir J* 2012;19(3): 209-215.

A previously validated computer model of the normal pulmonary circulation is adapted to simulate pulmonary arterial hypertension (PAH) in humans. Model predictions are used to explore the suitability of currently accepted criteria for diagnosing PAH by correlating hemodynamic data with the degree of vascular compromise (disease severity).

Model predictions demonstrate a hyperbolic relationship between vascular compromise, mean pulmonary artery pressure (PAPm) and pulmonary vascular resistance (PVR). PAPm and PVR change very little from disease initiation until a vascular compromise of 65% to 70% (surface area of 0.35 to 0.3 of baseline, respectively) is reached. Following that, further compromise is associated with a steep rise in PAPm and PVR.

The relationship between vascular compromise and hemodynamics may explain the relative stability of cardiac output early in this disease process and, therefore, the lack of symptoms. It also explains the rapid deterioration following diagnosis if the disease remains untreated.

Model predictions demonstrate the inadequacy of the current hemodynamic criteria for diagnosing PAH over a wide range of left atrial pressure and cardiac output combinations and for early detection of disease. The model provides an alternative approach to diagnosing PAH by translating hemodynamic data to degree of vascular compromise.

Key Words: *Computer model; Diagnostic criteria, Right heart catheterization*

Pulmonary arterial hypertension (PAH) belongs to group 1 in the most recent WHO classification of pulmonary hypertension (1). This group is composed of diseases in which the primary abnormality is located in the small pulmonary arteries. From the time of diagnosis, if left untreated, PAH deteriorates rapidly and is associated with a very poor prognosis, with a median survival of 2.8 years (five-year survival rate 34%) (2). Although recent treatment developments have offered improvements in hemodynamics, quality of life, time to clinical worsening and survival, compared with historical controls, prognosis remains poor (1). These poor outcomes have been attributed to the lack of curative treatment and to the long delay between disease initiation and detection (3).

Presently, the diagnosis of PAH is confirmed by right heart catheterization (4). PAH is recognized to be present when the mean pulmonary artery pressure (PAPm) is ≥ 25 mmHg, provided that pulmonary capillary wedge pressure (PCWP) is ≤ 15 mmHg (5).

A computer model was previously used to study the characteristic behaviour of the pulmonary circulation and attributed most of the nonlinearity in the PAPm-cardiac output (CO) and left atrial pressure (LAP)-PAPm relationships to vascular distensibility (6,7). This characteristic behaviour of the pulmonary circulation may have a significant impact on achieving the diagnostic criteria of PAH under a wide range of CO and LAP. For example, in the setting of a normal CO, a preserved vascular distensibility (upstream from the disease area) may cause a significant drop in upstream resistance, thus attenuating the rise in total pulmonary vascular resistance (PVR) and PAPm.

The goal of the present study was to assess the impact of progressive vascular compromise on pulmonary hemodynamics and to estimate the level of vascular compromise needed to achieve the current

L'atteinte vasculaire et l'hémodynamique en cas d'hypertension artérielle pulmonaire : prédictions d'un modèle

Un modèle informatique auparavant validé de la circulation pulmonaire normale est adapté pour stimuler l'hypertension artérielle pulmonaire (HAP) chez les humains. Les prédictions de ce modèle sont utilisées pour explorer la pertinence des critères actuellement acceptés pour diagnostiquer l'HAP en corrélant les données hémodynamiques au degré d'atteinte vasculaire (gravité de la maladie).

Les prédictions des modèles démontrent une relation hyperbolique entre l'atteinte vasculaire, la tension artérielle pulmonaire moyenne (TaPm) et la résistance vasculaire pulmonaire (RVP). La TaPm et la RVP changent très peu entre l'apparition de la maladie et une atteinte vasculaire de 65 % à 70 % (aire de la surface de 0,35 à 0,3 par rapport aux données de base, respectivement). Par la suite, une aggravation de l'atteinte s'associe à une augmentation abrupte de la TaPm et de la RVP.

Le lien entre l'atteinte vasculaire et l'hémodynamique peuvent expliquer la stabilité relative du débit cardiaque au début du processus de la maladie et, par conséquent, l'absence de symptômes. Il explique également la détérioration rapide après le diagnostic si la maladie demeure non traitée.

Les prédictions du modèle démontrent la déficience des critères hémodynamiques actuels pour diagnostiquer l'HAP par diverses combinaisons de pression auriculaire gauche et de débit cardiaque et pour dépister rapidement la maladie. Le modèle fournit une autre approche pour diagnostiquer l'HAP en traduisant les données hémodynamiques en degré d'atteinte vasculaire.

diagnostic criteria of PAH. Assessing the level of vascular compromise, even in experimental animals, is difficult and, hence, one must rely on modelling. In the present study, a previously validated computer model of the normal pulmonary circulation is adapted both to humans and to the simulation of PAH. PAPm and PVR, for a given level of vascular compromise, were generated over a wide range of LAPs and COs. The level of vascular compromise needed to establish the diagnosis of PAH using the current criteria is then determined. Over the wide range of LAP and CO conditions, situations in which PAH is underdiagnosed, even in the presence of severe vascular compromise, are explored. Although PAH is mostly a disease of proliferation rather than vasoconstriction, the impact of vasoconstriction on the results is also being explored.

METHODS

Pulmonary circulation model

A computer model of the normal pulmonary circulation based on animal (dog) data obtained in the literature was previously developed by Bshouty and Younes (6,7). Model development, adaptation to humans and simulation of PAH are briefly described in the online supplementary material (www.pulsus.com) and only details not included in the original model development (6,7) are included. The model is a multibranch model that bifurcates sequentially starting from the pulmonary artery (PA) up to sixteen precapillary and capillary channels (Figure 1). On the venous side, the vessels converge and reunite to end in the left atrium (LA). Although the model has only five generations, each generation in the model represents three generations in the human lung. Furthermore, each vessel within a generation represents thousands of vessels in a given generation (in the

Section of Respiratory Diseases, Department of Medicine, University of Manitoba, Winnipeg, Manitoba

Correspondence and reprints: Dr Zoheir Bshouty, RS317 Respiratory Hospital, Health Sciences Centre, 810 Sherbrook Street, Winnipeg, Manitoba R3A 1R8. Telephone 204-787-1059, fax 204-787-1433, e-mail zbshouty@hsc.mb.ca

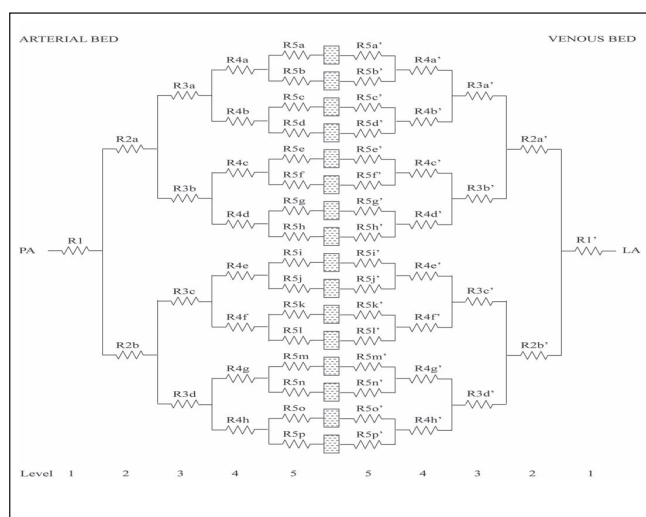


Figure 1) Multibranch model of the pulmonary circulation. The dashed rectangles in the centre represent the capillary bed. Left of the capillary bed is the arterial system. Starting with the pulmonary artery (PA), the arterial system bifurcates sequentially to form five arterial generations (up to 16 parallel channels). Right of the capillary bed the pulmonary venous system recombines sequentially ending in the left atrium (LA)

human lung) at the same hydrostatic level (For further details and justification of this aspect of the model, please see the online supplementary material and Discussion).

The baseline resistance of each vessel in each generation is assigned under standardized conditions (transpulmonary pressure [P_{tp}] of zero and vessel transmural pressure [P_{tm}] of 35 cmH₂O) and adjusted automatically to accommodate different patients' heights and weights. The operator enters three groups of data (general, patient specific and hemodynamic) into the model. General data include the reference point for pressure measurement (top or bottom of the lung, or LA) and the tolerance (accuracy) level for a given run (see online supplementary material). Patient-specific data include patient height, weight, lung height, lung compliance and lung volume at a $P_{tp}=0$ (as a percentage of total lung capacity). Hemodynamic data include the point of measurement during the respiratory cycle (as determined by alveolar pressure [P_{al}] and pleural pressure [P_{pl}]), LAP and CO. The computer iterates to find a stable solution. The output includes the distribution of individual pulmonary vascular flows, arterial, capillary and venous resistances across the whole pulmonary circulation including summary data of PAPm, PVR, upstream (arterial), middle (capillary) and downstream (venous) resistances (for further details see online supplementary material).

Simulation protocols

All simulations in the present study were performed supine, with a lung height of 20 cm at $P_{al}=0$, a $P_{pl}=-5$ cmH₂O (reflecting end-expiration) and a normal lung compliance (C_L) of 0.317 L/cmH₂O (8). All measurements were referenced to the LA hydrostatic level. The independent effect of LAP on establishing the diagnosis of PAH, at various degrees of vascular compromise (0% to 95%, in increments of 5%), was determined by generating PAPm and total PVR at a CO of 5 L/min with LA pressures ranging from 5 mmHg to 20 mmHg (in increments of 5 mmHg). The term 'compromise' is used here rather than 'narrowing' because the distensibility of the vessels is also affected with the progressive loss of cross-sectional area and disease progression (for further details see online supplementary material). The independent effect of CO on establishing the diagnosis of PAH at various degrees of vascular compromise was determined by generating PAPm and total PVR at a LAP of 7.5 mmHg with cardiac outputs ranging from 3 L/min to 6 L/min (in increments of 1 L/min). As mentioned

above, simulation data are examined against current criteria for establishing the diagnosis of PAH (a PAPm ≥ 25 mmHg in the presence of a PCWP [a reflection of LAP] ≤ 15 mmHg) (5).

Initially, simulations with only compromise of the fifth arterial generation vessels were generated. To assess the effect of vasoconstriction (smooth muscle tone) alone, and of vasoconstriction with proliferation on the characteristic behaviour of the pulmonary circulation, simulations with only vasoconstriction (either fourth or fifth arterial generation vessels, or both generations), followed by both vasoconstriction and compromise (fifth arterial generation) were generated. Vasoconstriction was applied equally throughout the arterial generation that is being explored. These simulations were limited to a CO of 5 L/min and a LAP of 10 mmHg.

It is important to mention that the present article presents a theoretical analysis that may encompass hemodynamic data, which may or may not be encountered in clinical practice. In addition, none of the figures shown in the Results section represents a continuum of observations in any given patient.

RESULTS

Simulation data of PAPm (left y-axis) and total PVR (right y-axis) as a function of cross-sectional area (percentage of baseline), at a CO of 5 L/min and LA pressures of 5, 10, 15, and 20 mmHg are shown in Figures 2A to 2D, respectively. Note that, irrespective of LAP, the relationship between PVR and area is curvilinear (hyperbolic), which is a result of the characteristic behaviour (recruitment and distensibility) of the pulmonary circulation (dashed-dotted lines in Figures 2A to 2D). For a given PVR, because the relationship between PAPm and LAP is linear, the relationship between PAPm and area is also hyperbolic (dashed lines in Figures 2A to 2D). From these relationships, it is evident that, starting with normal vessels and down to a vascular compromise of 70% (area = 30% of baseline), PAPm and PVR rise very little over a large range of LA pressures at a fixed CO (Figures 2A to 2D). Between 70% and 85% vascular compromise (area = 30% to 15% of baseline), a steeper rise in PAPm and PVR is seen. At a vascular compromise $>85\%$ (area $<15\%$ of baseline), the rise in PAPm and PVR becomes very steep. At LA pressures >15 mmHg (LAP of 20 mmHg, Figure 2D), the diagnosis of PAH cannot be considered irrespective of PAPm because of the requirement that PCWP be ≤ 15 mmHg.

Simulation results of PAPm and total PVR as a function of cross-sectional area at a LAP of 7.5 mmHg and cardiac outputs of 3, 4, 5 and 6 L/min are shown in Figures 3A to 3D, respectively. Again, notice that irrespective of CO, the relationships between both PVR and PAPm, and area are also hyperbolic. Also notice that irrespective of CO, over a large range of vascular compromise, PAPm and PVR rise very little, followed initially by a steeper and later by a very steep rise in both parameters. Because LAP in these simulations (LAP=7.5 mmHg) is <15 mmHg, this criterion does not interfere with the diagnosis of PAH.

To assess the potential for underdiagnosing patients with significant vascular compromise, PAPm data were generated at a vascular compromise of 80% (area = 20% of baseline) as a function of LAP and CO. The data is presented in Figures 4A and 5A, respectively. In this type of presentation, diagnosis is established when the dashed line (PAPm) is above the horizontal (solid) line (diagnosis threshold) and LAP is ≤ 15 mmHg (left of the solid vertical line in Figure 4). It is apparent from Figure 4A (CO of 5 L/min and vascular compromise of 80%, area = 20% of baseline) that all patients with LAPs ≤ 15 mmHg would be diagnosed with PAH (left of the solid vertical line). Of course, at LAPs >15 mmHg (right of the vertical line, Figure 4A), none of these patients would be diagnosed with PAH in spite of the severity of vascular compromise (here 80%). In Figure 5A (LAP = 7.5 mmHg and vascular compromise of 80%, area = 20% of baseline), only patients with cardiac outputs >2.8 L/min would be diagnosed with PAH and none of the patients with cardiac outputs <2.8 L/min.

To simulate an attempt to diagnose patients at an earlier stage of their disease, similar data were generated at a vascular compromise of

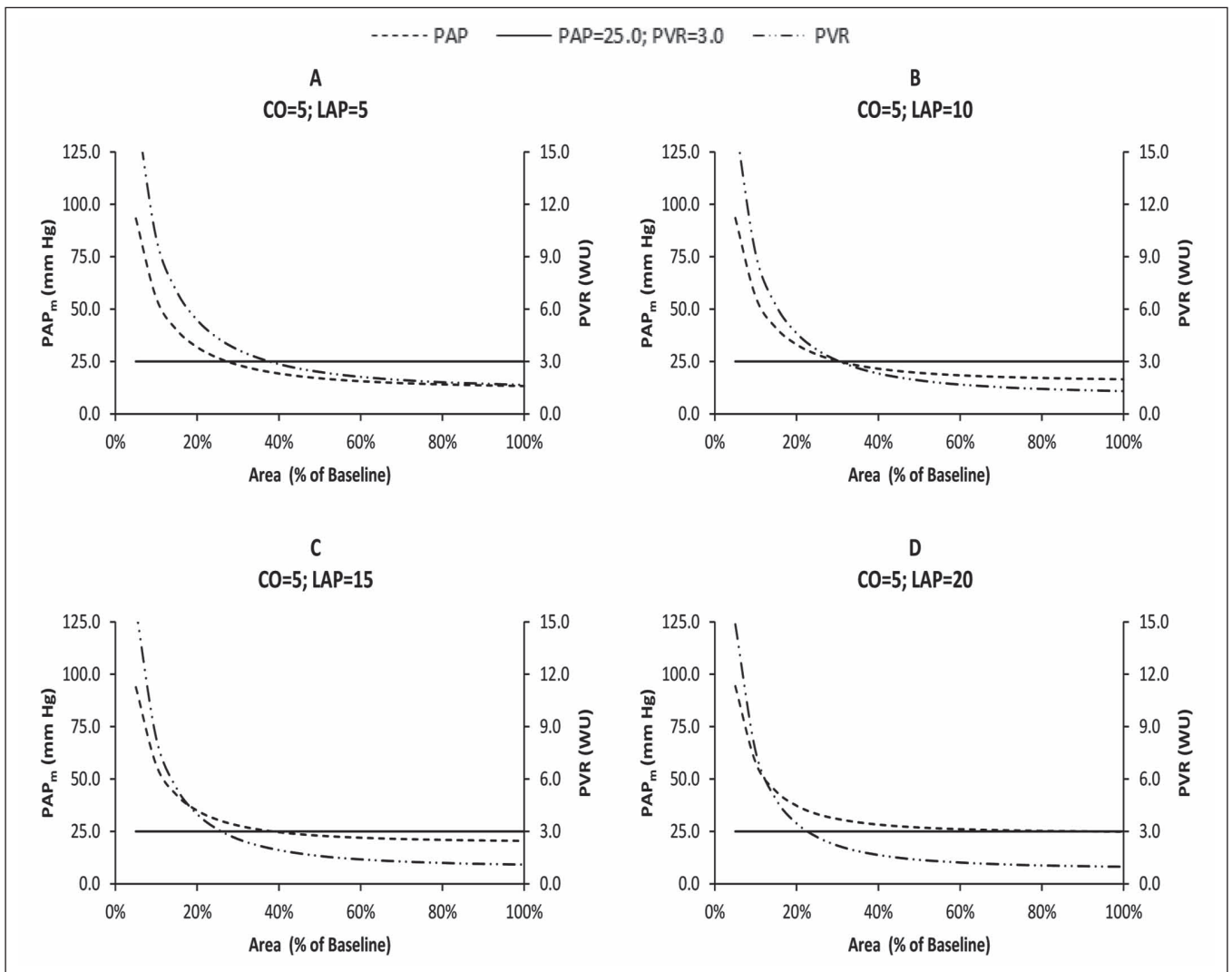


Figure 2) Correlation between mean pulmonary artery pressure (PAP_m; dashed lines, left y-axis), pulmonary vascular resistance (PVR; dashed-double dotted lines, right y-axis) and vascular compromise (as a per cent of baseline, x-axis) at a cardiac output (CO) of 5 L/min and left atrial pressures of 5 mmHg to 20 mmHg (in increments of 5 mmHg, panels A to D, respectively). Solid horizontal line represents the level above which PAP_m achieves the threshold for diagnosing pulmonary arterial hypertension, using currently accepted criteria

70% and 60% (areas of 30% and 40% of baseline, respectively). The results are represented in Figures 4B and 4C, and 5B and 5C. From Figure 4B, it is apparent that, using the current hemodynamic criteria, at a vascular compromise of 70% and CO of 5 L/min, only patients with LAP between 10 mmHg and 15 mmHg would be diagnosed with PAH and none of the patients with LAP <10 mmHg or >15 mmHg. Moreover, Figure 5B shows that at a LAP of 7.5 mmHg, only patients with a CO >5.5 L/min fulfill the criteria for diagnosis. It is apparent from Figure 4C that at a vascular compromise of 60%, none of the patients would be diagnosed with PAH over a wide range of LAPs because PAP_m exceeds 25 mmHg only at LAP >15 mmHg. Similarly, from Figure 5C, none of the patients would be diagnosed with PAH over a wide range of CO because PAP_m fails to exceed 25 mmHg.

Impact of smooth muscle tone on model predictions

To establish at what level of vasoconstriction (without vascular compromise) the diagnostic criteria for PAH are met, increasing levels of vasomotor tone were applied equally to the fourth arterial generation alone, the fifth arterial generation alone and both arterial generations. At a CO of 5 L/min and LAP of 10 mmHg, the criteria for diagnosing PAH were met only when vasoconstriction >24.5 mmHg was applied equally throughout the fifth arterial generation. At a CO of 5 L/min

and LAP of 10 mmHg, the criteria for diagnosing PAH were met only when applied vasoconstriction throughout the fourth arterial generation exceeded 27.1 mmHg. When vasomotor tone was applied to both fourth and fifth arterial generations, the criteria for diagnosing PAH were met only when applied vasoconstriction exceeded 22.4 mmHg (again, at a CO of 5 L/min and LAP of 10 mmHg). When applying vasomotor tone to every other vessel in either the fourth or the fifth arterial generation, the criteria for diagnosing PAH were not met, irrespective of the level of vasomotor tone. The same was true when every other vessel was completely occluded (equivalent to a pneumonectomy). Occlusion of every other fifth arterial generation vessel caused a rise in PAP_m and PVR from 16.52 mmHg and 1.30 mmHg/L/min (Wood Units, WU) to 19.13 mmHg and 1.83 WU, respectively. Figure 6 shows simulation results of PAP_m and PVR at a CO of 5 L/min and LAP of 10 mmHg, with and without vasoconstriction of 10 mmHg applied equally throughout the fifth arterial generation. As apparent from Figure 6, vasoconstriction shifts the PAP_m curve as a function of vascular compromise to the right. As a result, in the presence of vasoconstriction of 10 mmHg, the criteria for diagnosing PAH are met at a lower level of vascular compromise (60% with vasoconstriction compared with 70% without vasoconstriction, in this example). Although not shown, higher levels of vasoconstriction lead to a more pronounced right shift in the PAP_m curve.

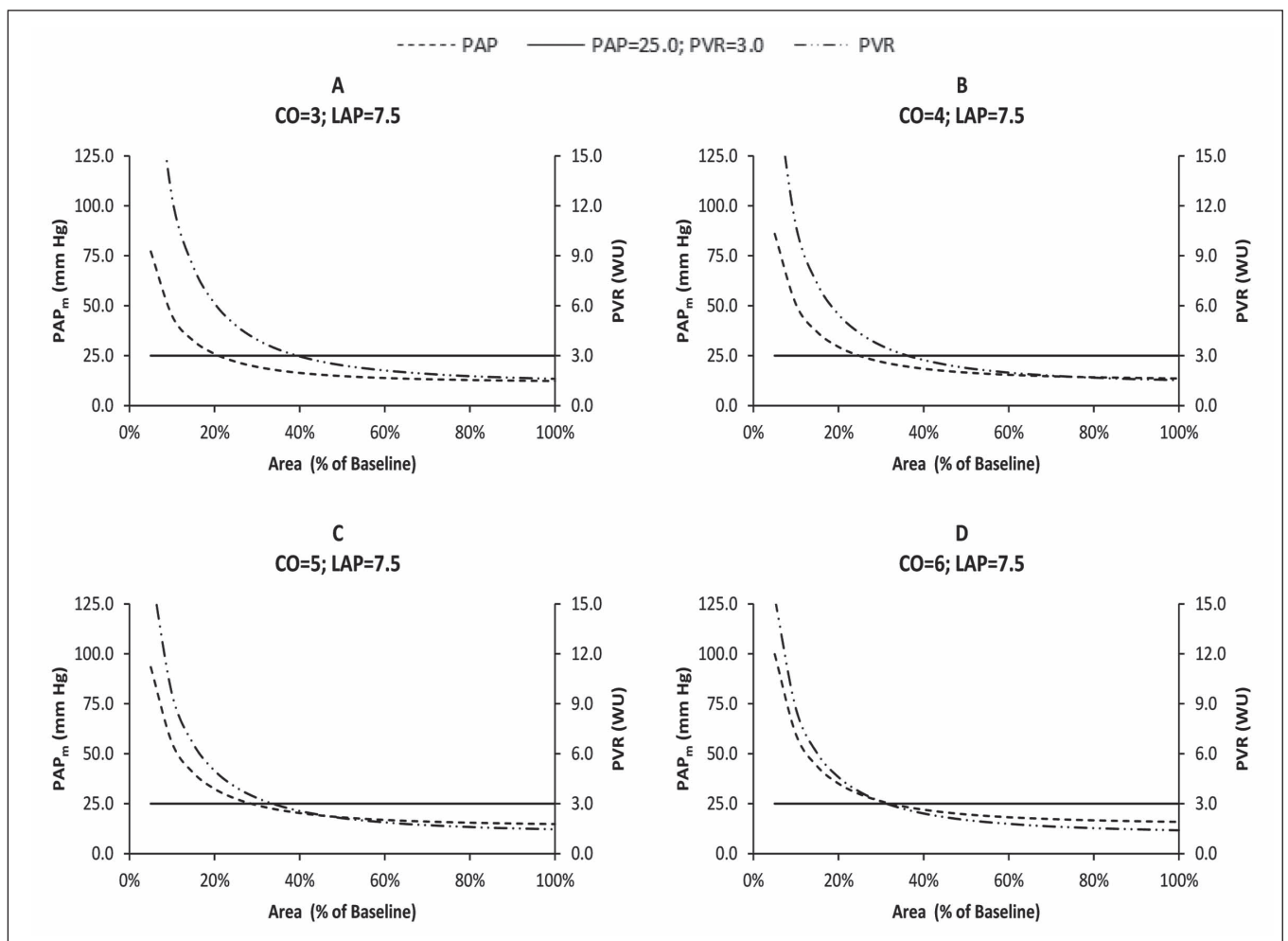


Figure 3 Correlation between mean pulmonary artery pressure (PAP_m, dashed lines, left y-axis), pulmonary vascular resistance (PVR; dashed-double dotted lines, right y-axis) and vascular compromise (as a per cent of baseline, x-axis) at a left atrial pressure (LAP) of 7.5 cmH₂O and cardiac outputs (CO) 3 L/min to 6 L/min (in increments of 1 L/min, panels A to D, respectively). Solid horizontal line represents the level above which PAP_m achieves the threshold for diagnosing pulmonary arterial hypertension, using currently accepted criteria

DISCUSSION

Modelling is an important tool that enables the study of the impact of individual components within a system on the total behaviour of a system. Using modelling, all components of the system and their behaviour under different conditions are accessible and measurable. This is often not available in vivo, either because of inability to access and measure certain components within a system, or the inability to control the experimental conditions to such an accurate extent to draw meaningful conclusions. However, for predictions to be trustworthy, model creation must be based, as much as possible, on physiological data obtained in vivo, and model predictions should be physiologically sound and reproduce data obtained in real life under measurable conditions. This model of the pulmonary circulation was created using these principles. Although not all possible factors (such as pulsatile flow and continuous breathing) were accounted for, as many factors as physiologically and mathematically possible were included. The original model was created based on data obtained in dogs and was validated by comparing model predictions (PAP_m-Flow and PAP_m-LAP relationships) with animal data obtained under similar conditions (7).

Representing fifteen generations of arterial and venous vessels in a five-generation model was achieved by grouping every three generations in the real lung to one generation in the model. This grouping is justified by data in the literature, which showed that the distensibility of the pulmonary arterial bed is equal across generations and is

independent of vessel diameter (9-12). Similar findings were observed in the pulmonary venous bed (13). Adaptation of the model to humans, and later to PAH, was achieved by using reasonable assumptions. Given the similar histological structure of pulmonary arteries, veins and capillaries in both humans and dogs, it is conceivable that the characteristic behaviour (transmural pressure cross-sectional area relationships) of these structures is similar in both species and, therefore, this was assumed in the present study. Although the model branching is dichotomous, resistance of each vessel in the model represented the cumulative resistances of three generations in the human lung at the same hydrostatic level. The longitudinal distribution of pulmonary vascular resistance along the vascular bed was not random but was based on data obtained in humans by Huang et al (14) and took into account parent to daughter vessel diameter and length ratios (for further details, please see the online supplementary material).

Lung compliance in the model is an independent variable that correlates changes in P_{tp} with lung volume. Lung volume, in turn, affects vascular characteristics (both length and cross sectional area) through stretching (vessel length) and through its effect on perivascular pressure (and hence, vessel cross-sectional area). Lung compliance in the current simulations was assumed equal to that in the normal human.

In adapting the model to represent PAH, it was assumed that the disease is that of small precapillary arteries. All other vessels were assumed to be normal. This was based on the pathological knowledge of this disease (15). In addition, it was assumed that the disease is

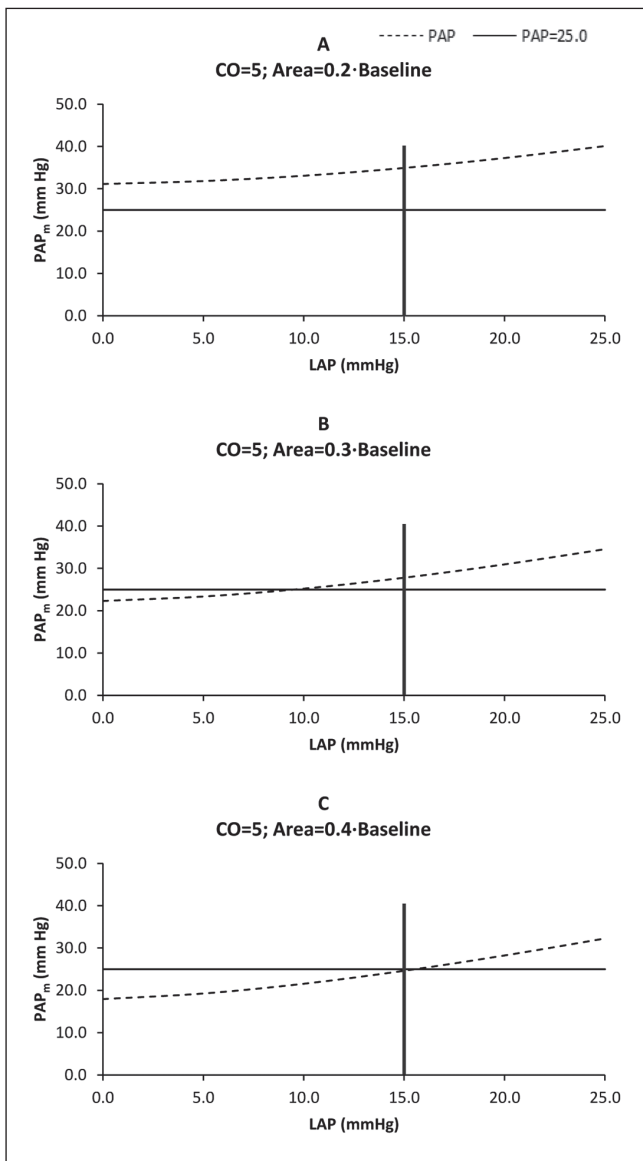


Figure 4) Correlation between mean pulmonary artery pressure (PAP_m; dashed line) and left atrial pressure (LAP) (x-axis) at a cardiac output of 5 L/min and a vascular compromise of 80% (A), 70% (B) and 60% of baseline (C). Solid horizontal line represents the level above which PAP_m achieves the threshold for diagnosing pulmonary arterial hypertension, provided that LAP is ≤15 mmHg (left of solid vertical line)

diffuse and homogeneous (16). The introduction of inhomogeneity would have attenuated the rise in PAP_m and PVR even further, in which case the diagnosis of PAH would have been established at a greater level of vascular compromise than what is described in the present article. In addition, in the presence of inhomogeneity, disease severity is difficult to quantify and define accurately. Furthermore, one may view these predictions of vascular compromise as a concept similar to the concept of shunt. For example, when shunt is 12%, it is as if 12% of the pulmonary circulation is bypassing oxygenated alveoli, causing the blood flowing through these regions to remain venous while the rest of the blood flow is adequately oxygenated. When in reality, oxygenation in the millions of alveolar-vascular units, throughout the lung, ranges between the two extremes. Similarly, when the model predicts a vascular compromise of 70% for a given set of hemodynamic data, the interpretation of such a prediction is that if the disease were to be applied diffusely and equally to the precapillary

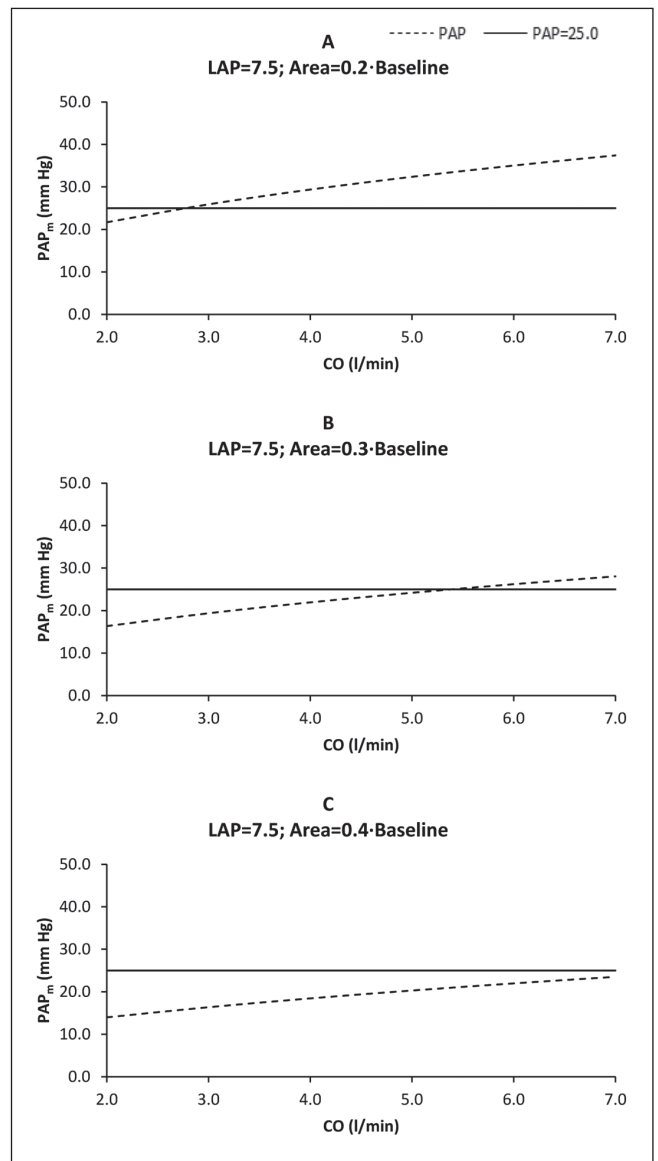


Figure 5) Correlation between mean pulmonary artery pressure (PAP_m; dashed line) and cardiac output (CO) (x-axis) at a left atrial pressure (LAP) of 7.5 mmHg and a vascular compromise of 80% (A), 70% (B), and 60% of baseline (C). Solid line represents the level above which PAP_m achieves the threshold for diagnosing pulmonary arterial hypertension. When the dashed line is above the solid line, currently accepted criteria for diagnosing pulmonary arterial hypertension are met

arteries, it is as if the total cross-sectional area of these vessels is down to 30% of normal. Translating hemodynamic data into vascular compromise (disease severity) enables one to compare two or more sets of hemodynamic data obtained, either in the same patient (over time), or in multiple patients (or groups of patients), with regard to disease severity and progression.

If one assumes that vascular compromise progresses linearly as a function of time, then model predictions may explain the long delay between disease initiation and symptom development (flat portion of PVR as a function of cross-sectional area in Figures 2 and 3). The preserved CO over the same range of vascular compromise, in turn, explains the delay in symptom development. At a critical point in the disease progression, the rise in PVR becomes steeper (notice the more rapid rise in PVR at a vascular compromise between 70% and 85%, Figures 2 and 3). The latter may also explain the rapid deterioration in

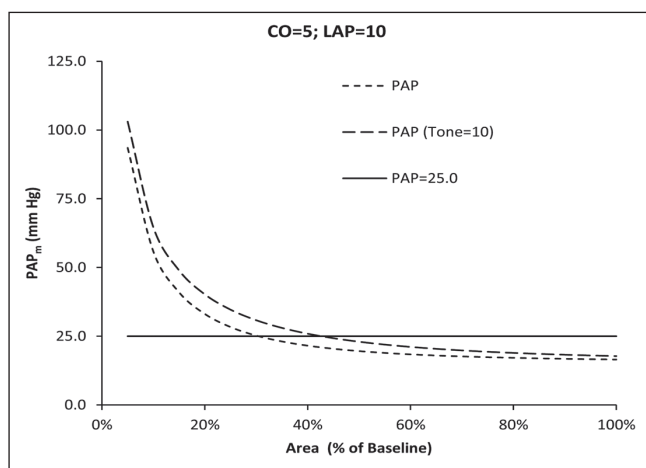


Figure 6 Correlation between mean pulmonary artery pressure (PAP_m; y-axis) and vascular compromise (as per cent of baseline, x-axis) at a cardiac output (CO) of 5 L/min and left atrial pressures of 10 mmHg without (dashed line) and with (long-dashed line) vasoconstriction of 10 mmHg (Tone=10). Solid horizontal line represents the level above which PAP_m achieves the threshold for diagnosing pulmonary arterial hypertension

hemodynamics and, in turn, functional status of patients following their diagnosis if the disease remains untreated. At a vascular compromise >85%, the rise in PVR is very steep, representing a significantly vulnerable period of rapid decompensation leading to death soon after (Figures 2 and 3). Correlations between model predictions of vascular compromise at time of diagnosis and outcome, and between changes in vascular compromise (in response to treatment) over time are currently underway.

As shown in Figure 4A, at a vascular compromise of 80%, all patients with LAP ≤15 mmHg would be diagnosed with PAH and none of the patients with LAP >15 mmHg. Yet, excluding these patients completely would be unreasonable. It is not uncommon to have patients with PAH who have a PCWP or left ventricular end-diastolic pressure (LVEDP) >15 mmHg. These patients are often recognized as having PA pressures that are elevated to a degree that is out of proportion to the rise in LAP. This may happen in patients who, in addition to suffering from PAH, also suffer from other conditions that may cause left ventricular dysfunction (eg, systemic hypertension with left ventricular hypertrophy or a component of left ventricular diastolic dysfunction secondary to underlying ischemic heart disease). It is also conceivable that in severe disease, with progressive dilation of the right ventricle and deviation of the interventricular septum to the left, compromise of left ventricular filling develops, causing LVEDPs and, in turn, LA pressures to rise to levels >15 mmHg even in the absence of intrinsic left ventricular dysfunction (17). How can we justify offering treatment to one subject with all the clinical features of PAH whose PAP_m is 60 mmHg and whose PCWP is 15 mmHg and deny another with the same clinical features and hemodynamic data except for a PCWP of 16 mmHg? It is worth mentioning that the hemodynamic criteria for diagnosing PAH have undergone multiple revisions since the study by Rich et al (18). Neither the original nor the revised criteria, were ever validated. Yet, we continue to use them as the gold standard for diagnosis.

In the study by McIntyre et al (19), rat PA rings (2 mm to 3 mm in length and 2 mm to 3 mm in external diameter) were exposed to several vasoconstrictive substances. Maximal tension was achieved with potassium chloride and was in the range of 550 mg. A specimen 2 mm long with an external diameter of 2 mm and a generated tension of 600 mg translates into a perpendicular force of approximately 20 mmHg. From our results, fulfilling the diagnostic criteria of PAH by vasoconstriction alone required a perpendicular force of 24.5 mmHg applied equally over the entire fifth arterial generation and 22.4 mmHg when

applied over the entire fourth and fifth arterial generations. Hence, from our results, under normal CO and LAP, vasoconstriction alone is unlikely to establish a diagnosis of PAH unless it is at its maximal level. Also as shown in the results, applying vasoconstriction to 50% of the fifth arterial generation or even complete occlusion of these vessels (equivalent to a pneumonectomy) does not cause hemodynamic compromise. As shown in Figure 6, the presence of a moderate level of vasoconstriction allows the diagnosis of PAH to be established at a lower level of vascular compromise. This type of behaviour may explain the improved survival of PAH patients who are vasoresponsive to the acute administration of a short-acting vasodilator at the time of right heart catheterization. This survival benefit may be merely the result of time bias rather than a true intervention effect at an earlier stage of the disease.

In the absence of vasoconstriction, the current hemodynamic criteria for diagnosing PAH are completely inadequate if the diagnosis is to be established at a vascular compromise of 60% (Figures 4C and 5C) or even 70% (Figures 4B and 5B). As mentioned above, an alternative approach would be to use the model in the reverse order. Using this approach, patient height, weight, lung height in the supine position, estimates of lung volume at a $P_{tp}=0$ (per cent of total lung capacity), lung compliance, alveolar and pleural pressures at end-expiration, and hemodynamic measurements (LAP, CO and PAP_m), are entered into the model. The model iterates to derive the degree of vascular compromise associated with these parameters. This approach is more consistent in providing disease severity especially when the possible combinations of hemodynamic measurements are endless and can be affected by conditions as simple as the level of hydration. In this fashion, rather than assessing disease severity by hemodynamic parameters, which are quite insensitive over a large range of disease severity, disease severity is assessed by the degree of vascular compromise. Furthermore, this approach may be applied to asymptomatic patients who are at a higher risk of developing PAH.

SUMMARY

The characteristic behaviour of the pulmonary circulation, dictates nonlinearities between vascular compromise and PVR. Starting with a normal pulmonary arterial precapillary bed down to a vascular compromise of 30% of baseline, PAP_m rises very little, preventing the achievement of currently accepted criteria for diagnosing PAH. The insensitivity of hemodynamic data to disease progression may explain the delay in diagnosing many patients with PAH. The steep portion of the relationship between PVR and cross-sectional area may also explain the rapid deterioration of patients following diagnosis in whom the disease remains untreated. The current hemodynamic criteria are inadequate for diagnosing PAH under a wide range of CO and LAP conditions at an estimated vascular compromise of 70% and completely inadequate at milder levels of the disease. Using model predictions in reverse order, hemodynamic data are translated into vascular compromise, a concept similar to shunt, which enables us to quantify disease severity. Vascular compromise may enable us to follow patients over time (with regard to disease progression) or compare different groups of patients with a wide range of hemodynamic data (with regard to disease severity).

REFERENCES

- McLaughlin VV, Archer SL, et al; American College of Cardiology Foundation Task Force on Expert Consensus Documents; American Heart Association; American College of Chest Physicians; American Thoracic Society, Inc; Pulmonary Hypertension Association. J Am Coll Cardiol 2009;53:1573-619.
- D'Alonzo GE, Barst RJ, Ayres SM, et al. Survival in patients with primary pulmonary hypertension. Results from a national prospective registry. Ann Intern Med 1991;115:343-9.
- Humbert M. Update in pulmonary arterial hypertension 2007. Am J Respir Crit Care Med 2008;177:574-9.

4. Sitbon O, Humbert M, Jaïs X, et al. Long-term response to calcium channel blockers in idiopathic pulmonary arterial hypertension. *Circulation* 2005;111:3105-11.
 5. Galiè N, Hoepfer M, Humbert M, et al. Guidelines for the diagnosis and treatment of pulmonary hypertension. The Task Force for the Diagnosis and Treatment of Pulmonary Hypertension of the European Society of Cardiology (ESC) and the European Respiratory Society (ERS) endorsed by the International Society of Heart and Lung Transplantation (ISHLT). *Eur Respir J* 2009;34:1219-63.
 6. Bshouty Z, Younes M. Distensibility and pressure-flow relationship of the pulmonary circulation. I. Single-vessel model. *J Appl Physiol* 1990;68:1501-13.
 7. Bshouty Z, Younes M. Distensibility and pressure-flow relationship of the pulmonary circulation. II. Multibranching model. *J Appl Physiol* 1990;68:1514-27.
 8. Galetke W, Feier C, Muth T, Ruehle KH, Borsch-Galetke E, Randerath W. Reference values for dynamic and static pulmonary compliance in men. *Respir Med* 2007;101:1783-9.
 9. Cox RH. Comparison of mechanical and chemical properties of extra- and intralobar canine pulmonary arteries. *Am J Physiol* 1982;242:H245-53.
 10. al-Tinawi A, Madden JA, Dawson CA, Linehan JH, Harder DR, Rickaby DA. Distensibility of small arteries of the dog lung. *J Appl Physiol* 1991;71:1714-22.
 11. Karau KL, Molthen RC, Dhyani A, et al. Pulmonary arterial morphometry from microfocal X-ray computed tomography. *Am J Physiol Heart Circ Physiol* 2001;281:H2747-56.
 12. Molthen RC, Karau KL, Dawson CA. Quantitative models of the rat pulmonary arterial tree morphometry applied to hypoxia-induced arterial remodeling. *J Appl Physiol* 2004;97:2372-84.
 13. al-Tinawi A, Clough AV, Harder DR, Linehan JH, Rickaby DA, Dawson CA. Distensibility of small veins of the dog lung. *J Appl Physiol* 1992;73:2158-65.
 14. Huang W, Yen RT, McLaurine M, Bledsoe G. Morphometry of the human pulmonary vasculature. *J Appl Physiol* 1996;81:2123-33.
 15. Palevsky HI, Schloo BL, Pietra GG, et al. Primary pulmonary hypertension. Vascular structure, morphometry, and responsiveness to vasodilator agents. *Circulation* 1989;80:1207-21.
 16. Pietra GG, Capron F, Stewart S, et al. Pathologic assessment of vasculopathies in pulmonary hypertension. *J Am Coll Cardiol* 2004;43:25S-32S.
 17. Morris-Thurgood JA, Frenneaux MP. Diastolic ventricular interaction and ventricular diastolic filling. *Heart Fail Rev* 2000;5:307-23.
 18. Rich S, Dantzker DR, Ayres SM, et al. Primary pulmonary hypertension. A national prospective study. *Ann Intern Med* 1987;107:216-23.
 19. McIntyre RC Jr, Agrafojo J, Banerjee A, Fullerton DA. Pulmonary vascular smooth muscle contraction. *J Surg Res* 1996;61:170-4.
-